VIP *The following Communications have been judged by at least two referees to be "very important papers" and will be published online at www.angewandte.org soon:*

*T. Lewis, M. Faubel, B. Winter, J. C. Hemminger**
CO_2 Capture in an Aqueous Solution of an Amine: Role of the Solution Interface

*Y. H. Kim, S. Banta**
Complete Oxidation of Methanol in an Enzymatic Biofuel Cell by a Self-Assembling Hydrogel Created from Three Modified Dehydrogenases

A. Bonet, C. Pubill-Ulldemolins, C. Bo, H. Gulyás,* E. Fernández**
Transition-Metal-Free Diboration by the Activation of Diboron Compounds with Simple Lewis Bases

*M. Nakanishi, D. Katayev, C. Besnard, E. P. Kündig**
Synthesis of Fused Indolines by Palladium-Catalyzed Asymmetric C–C Coupling Involving an Unactivated Methylene Group

A. W. Fay, M. A. Blank, C. C. Lee, Y. Hu, K. O. Hodgson,* B. Hedman,* M. W. Ribbe**
Spectroscopic Characterization of a Precursor Isolated from NifEN of an Iron–Molybdenum Cofactor

P. G. Cozzi, A. Gualandi, E. Emer, M. G. Capdevila*
Highly Enantioselective α Alkylation of Aldehydes with 1,3-Benzodithiolylium Tetrafluoroborate: A General Formal Organocatalytic α Alkylation of Aldehydes by Carbenium Ions

*V. Zinth, T. Dellmann, H.-H. Klauss, D. Johrendt**
Recovery of a Parentlike State in $Ba_{1-x}K_xFe_{1.86}Co_{0.14}As_2$

*B. Purushothaman, M. Bruzek, S. R. Parkin, A.-F. Miller, J. E. Anthony**
Synthesis and Structural Characterization of Crystalline Nonacenes

D. Zhong, F. L. Sousa, A. Müller, L. Chi,* H. Fuchs**
Nanosized Molybdenum Oxide Wheel as a Unique Electronic Necklace: STM Study with Submolecular Resolution

*I. Coin, M. H. Perrin, W. W. Vale, L. Wang**
Photo-Cross-Linkers Incorporated into G-Protein-Coupled Receptors in Mammalian Cells: A Ligand Comparison

Author Profile

"My best investment was my education.
The best advice I have ever been given is 'Don't get bogged down in BS' …"
This and more about Vincent L. Pecoraro can be found on page 6696.

Meeting Reviews

Obituaries

Books

Contents

Minireviews

Brønsted Acid Catalysis

Chiral highly acidic Brønsted acids B*-H (see scheme, bottom) are efficient organocatalysts for numerous enantioselective reactions. Owing to their high acidity, these catalysts are suitable for the activation of imines, carbonyl compounds, and other weakly basic substrates. The formation of chiral contact-ion pairs (see scheme, top) implicates completely new modes of activation for asymmetric synthesis.

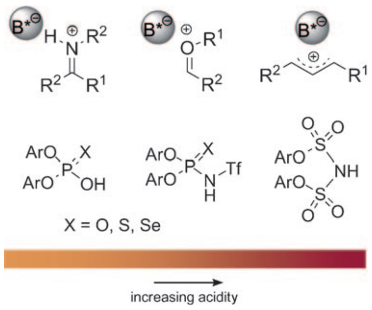

Reviews

Nobel Reviews

Tools for chemists: The Nobel Prize in Chemie 2010 was awarded for research on palladium-catalyzed cross-coupling in organic synthesis. Two of the Laureates, A. Suzuki and E. Negishi, report here first hand on the historical development and the current status of this research.

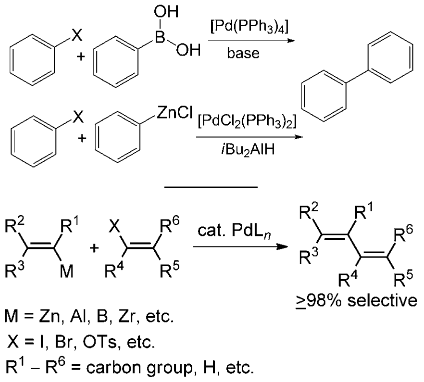

Communications

Contact Electrification

Was Thales right about water? Contrary to previous reports, contact charging can occur in the absence of water. At the same time, water helps stabilize the developed charges. Water-free conditions are realized by performing all experiments and charge measurements under oil-immersion.

For the USA and Canada:
ANGEWANDTE CHEMIE International Edition (ISSN 1433-7851) is published weekly by Wiley-VCH, PO Box 191161, 69451 Weinheim, Germany. Air freight and mailing in the USA by Publications Expediting Inc., 200 Meacham Ave., Elmont, NY 11003. Periodicals postage paid at Jamaica, NY 11431. US POSTMASTER: send address changes to *Angewandte Chemie*, Journal Customer Services, John Wiley & Sons Inc., 350 Main St., Malden, MA 02148-5020. Annual subscription price for institutions: US$ 9442/8583 (valid for print and electronic / print or electronic delivery); for individuals who are personal members of a national chemical society prices are available on request. Postage and handling charges included. All prices are subject to local VAT/sales tax.

theory loves reality

75.000

BASF inventions have become an integral part of our daily lives. By orienting themselves on the demands of the market, research teams are able to open up new business areas and continually achieve excellent results. When inventions are not only useful, but also marketable, it's because at BASF, we create chemistry.

BASF
The Chemical Company

Gas Release

H. Kim, J. Park, K. Noh, C. J. Gardner, S. D. Kong, J. Kim,* S. Jin* **6771 – 6775**

An *X–Y* Addressable Matrix Odor-Releasing System Using an On–Off Switchable Device

An olfactory factory: Using a novel polydimethylsiloxane (PDMS) elastomer-based device, the switchable release of specific gases is demonstrated. Heating elements trigger the gas release by warming the gas-containing capsule (see scheme). The release can be switched on and off by repeated thermal cycles. An *X–Y* addressable matrix of such capsules results in an odor-releasing system for multiple odors for virtual-reality applications.

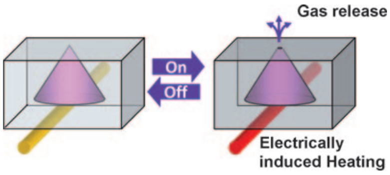

Post-Translational Modification

K. Liu, P.-Y. Yang, Z. Na, S. Q. Yao* **6776 – 6781**

Dynamic Monitoring of Newly Synthesized Proteomes: Up-Regulation of Myristoylated Protein Kinase A During Butyric Acid Induced Apoptosis

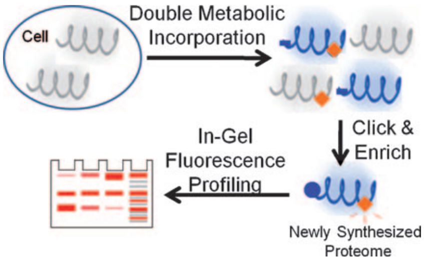

Doubly charged: A double metabolic incorporation approach capable of proteome-wide profiling of post-translational modification dynamics on newly synthesized proteins has been developed (see scheme; blue box: methionine surrogate, orange diamond: PTM probe). This strategy reveals for the first time that up-regulation of myristoylated PKA protein is necessary for the occurrence of butyric acid induced apoptosis in Jurkat cells.

Molecular Switches

H. Li, A. C. Fahrenbach, A. Coskun, Z. Zhu, G. Barin, Y.-L. Zhao, Y. Y. Botros, J.-P. Sauvage,* J. F. Stoddart* **6782 – 6788**

A Light-Stimulated Molecular Switch Driven by Radical–Radical Interactions in Water

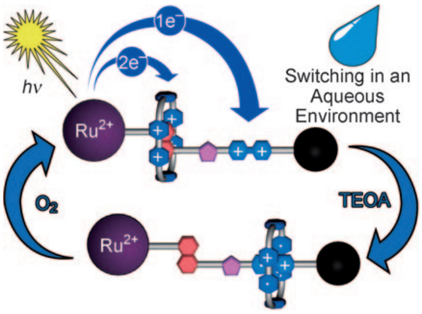

A redox-controllable bistable [2]rotaxane has been synthesized using templation and click chemistry. With assistance from a sacrificial electron donor, light-triggered switching through numerous cycles can be initiated by radical-pairing interactions between the reduced forms of the cyclophane and the bipyridinium unit in aqueous solution in the absence of air. In the presence of air (O_2), the interactions are reset by donor–acceptor charge transfer.

Plasmonic Nanoparticles

L. Zhang, Y. Li, D.-W. Li, C. Jing, X. Chen, M. Lv, Q. Huang, Y.-T. Long,* I. Willner ——— **6789 – 6792**

Single Gold Nanoparticles as Real-Time Optical Probes for the Detection of NADH-Dependent Intracellular Metabolic Enzymatic Pathways

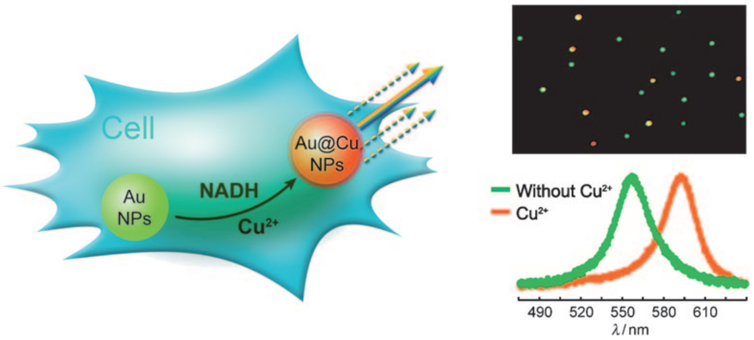

A coat of many colors: Plasmon resonance Rayleigh scattering (PRRS) spectroscopy is applied to the in-situ monitoring of the NADH-dependent growth of Au@Cu core–shell nanoparticles (NPs). The scattering signal of the AuNPs is red shifted when they are coated with Cu (see scheme). In conjunction with dark-field microscopy, a colorimetric NADH-dependent biosensor was constructed and tested to screen an anticancer drug affecting cell NADH metabolism.

Imaging Agents

R. Yan, E. El-Emir, V. Rajkumar, M. Robson, A. P. Jathoul, R. B. Pedley, E. Årstad* ——— **6793 – 6795**

One-Pot Synthesis of an ^{125}I-Labeled Trifunctional Reagent for Multiscale Imaging with Optical and Nuclear Techniques

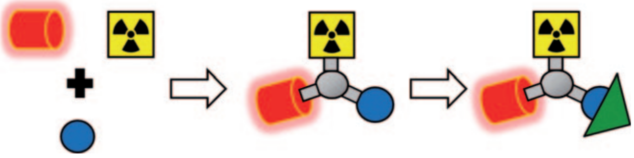

A highly efficient and rapid Cu^{II}-mediated three-component "click reaction" allows one-pot assembly of dual optical and nuclear labeling reagents. Proof-of-concept imaging studies demonstrate that the distribution of the dual-labeled antibody A5B7 can be interrogated from the cellular to the macroscopic level using a combination of optical and nuclear imaging techniques.

Asymmetric Synthesis

T. Kawasaki,* S. Kamimura, A. Amihara, K. Suzuki, K. Soai* ——— **6796 – 6798**

Enantioselective C–C Bond Formation as a Result of the Oriented Prochirality of an Achiral Aldehyde at the Single-Crystal Face upon Treatment with a Dialkyl Zinc Vapor

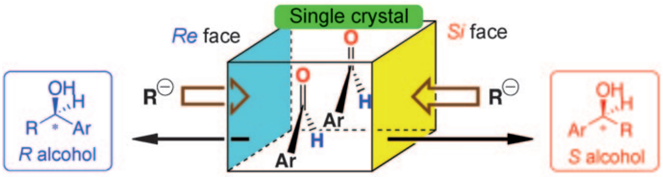

Show your best face: An achiral pyrimidine-5-carbaldehyde that forms an achiral crystal ($P\bar{1}$) with enantiotopic (001) and (00$\bar{1}$) faces underwent enantioselective addition of iPr$_2$Zn to the single exposed enantiotopic surface to give highly enantiomerically enriched S and R secondary alcohols (see scheme). The absolute configuration of the alcohol product correlated with the orientation of the prochiral aldehyde in the achiral crystal lattice.

Nanostructures

R. Liu, S. M. Mahurin, C. Li, R. R. Unocic, J. C. Idrobo, H. J. Gao, S. J. Pennycook, S. Dai* ——— **6799 – 6802**

Dopamine as a Carbon Source: The Controlled Synthesis of Hollow Carbon Spheres and Yolk-Structured Carbon Nanocomposites

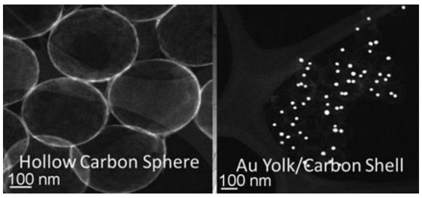

C shells: A facile and versatile synthesis using dopamine as a carbon source gives hollow carbon spheres and yolk–shell Au@Carbon nanocomposites (see pictures). The uniform nature of dopamine coatings and their high carbon yield endow the products with high structural integrity. The Au@C nanocomposites are catalytically active.

Contents

Asymmetric Catalysis

T. Goto, K. Takeda, N. Shimada, H. Nambu, M. Anada, M. Shiro, K. Ando, S. Hashimoto* ____________ **6803 – 6808**

Highly Enantioselective Cyclopropenation Reaction of 1-Alkynes with α-Alkyl-α-Diazoesters Catalyzed by Dirhodium(II) Carboxylates

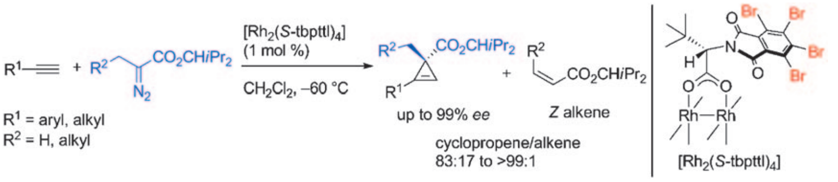

Two rhodium(II) ions work together: $[Rh_2(S\text{-tbpttl})_4]$ is an exceptionally effective catalyst for enantioselective cyclopropenation reactions of 1-alkynes with α-alkyl-α-diazoacetates (see scheme). Cyclopropenation is preferred over alkene formation through a 1,2-hydride shift.

Reaction Mechanisms

J. Kong, B. Galabov,* G. Koleva, J.-J. Zou,* H. F. Schaefer, III, P. von R. Schleyer* ________ **6809 – 6813**

The Inherent Competition between Addition and Substitution Reactions of Br_2 with Benzene and Arenes

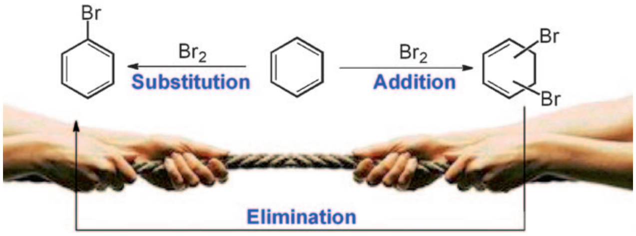

Tug of war: Comprehensive DFT computational exploration of the reaction mechanisms predicts that the barriers for Br_2 addition processes to benzene, naphthalene, anthracene, and phenanthrene in isolation (i.e., in the absence of catalysts, see picture) and in simulated CCl_4 solution can be even lower than the barriers for direct substitution. Moreover, substitution products also can arise from stepwise Br_2 addition–HBr elimination routes.

Natural Product Synthesis

J. J. Day, R. M. McFadden, S. C. Virgil, H. Kolding, J. L. Alleva, B. M. Stoltz* ______________ **6814 – 6818**

The Catalytic Enantioselective Total Synthesis of (+)-Liphagal

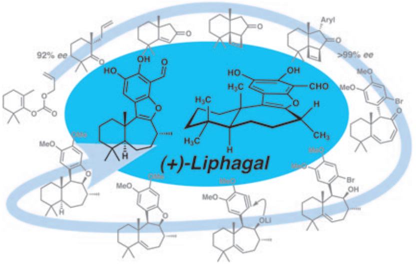

Ring a ding: The meroterpenoid natural product (+)-liphagal has been synthesized enantioselectively in 19 steps from commercially available materials. The *trans*-homodecalin system was achieved by ring expansion followed by stereoselective hydrogenation.

Single-Walled Carbon Nanotubes

G. Hong, M. Zhou, R. X. Zhang, S. M. Hou, W. M. Choi, Y. S. Woo, J. Y. Choi, Z. F. Liu, J. Zhang* ________________ **6819 – 6823**

Separation of Metallic and Semiconducting Single-Walled Carbon Nanotube Arrays by "Scotch Tape"

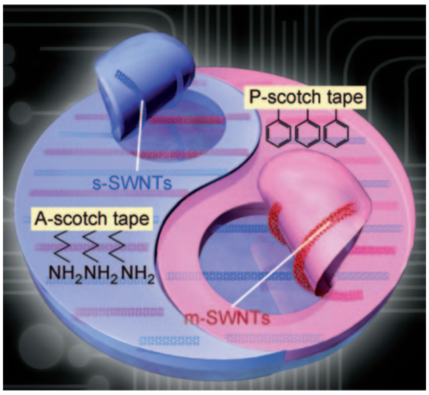

Peeling off nanotubes: Chemically modified soft polydimethylsiloxane (PDMS) thin films act as "scotch tape" for the separation of semiconducting (s) and metallic (m) single-walled carbon nanotubes (SWNTs). Whereas the amine-functionalized A-scotch tape selectively removed s-SWNTs, the phenyl-functionalized P-scotch tape acted specifically towards m-SWNTs (see picture). The resulting separation process is very gentle, no damage to the SWNTs was observed.

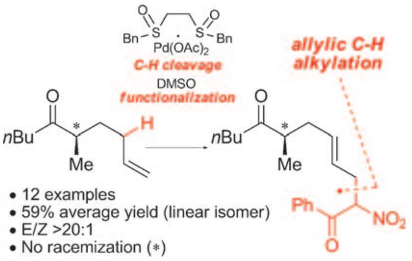

A delicate interplay of several kinetically labile ligands is required for reactions that proceed through serial ligand catalysis mechanisms. An investigation of the disruption of this balance has enabled the development of a method for the intermolecular allylic C—H alkylation of unactivated as well as activated α-olefins (see example, Bn = benzyl).

C—H Alkylation

A. J. Young, M. C. White* ___ **6824 – 6827**

Allylic C—H Alkylation of Unactivated α-Olefins: Serial Ligand Catalysis Resumed

---

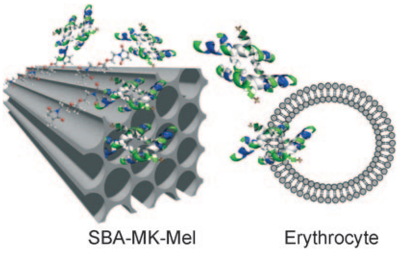

Free to go: A pH-labile immobilization of the melittin peptide with acetal linkers in the pore system of a SBA-15 host allows release of the peptide upon decrease of the pH value from 7.4 to 5.5. Such a release is shown by melittin-induced lysis of mouse erythrocytes. The method could be used to prepare new silica-based peptide delivery systems for targeted cancer therapy.

pH-Responsive Release

A. Schlossbauer, C. Dohmen, D. Schaffert, E. Wagner, T. Bein* ________ **6828 – 6830**

pH-Responsive Release of Acetal-Linked Melittin from SBA-15 Mesoporous Silica

---

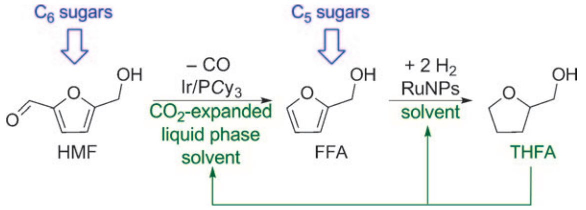

Less is more: The integrated development and optimization of catalysts and reaction media led to a highly selective decarbonylation of 5-(hydroxymethyl)furfural (HMF) to furfuryl alcohol (FFA) with an iridium/phosphine catalyst in the presence of compressed carbon dioxide. Subsequent hydrogenation over ruthenium nanoparticles (RuNPs) led to tetrahydrofurfuryl alcohol (THFA), a possible solvent for the decarbonylation reaction (see scheme).

Biomass

F. M. A. Geilen, T. vom Stein,
B. Engendahl, S. Winterle, M. A. Liauw,
J. Klankermayer,*
W. Leitner* ______________ **6831 – 6834**

Highly Selective Decarbonylation of 5-(Hydroxymethyl)furfural in the Presence of Compressed Carbon Dioxide

---

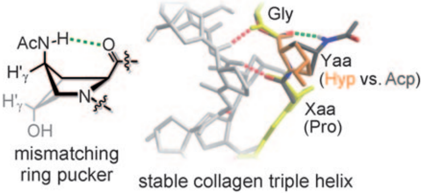

Mismatch is fine: Proline derivatives with a ring pucker mismatching that of natural collagen but with favorable torsional angles along the peptide chain are readily tolerated within the collagen triple helix (see picture). In contrast, a competition between intramolecular and interstrand H bonds destabilizes the collagen triple helix.

Collagen

R. S. Erdmann,
H. Wennemers* __________ **6835 – 6838**

Importance of Ring Puckering versus Interstrand Hydrogen Bonds for the Conformational Stability of Collagen

Gene Editing

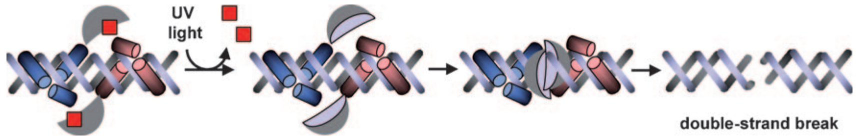

Light, zinc-finger nuclease, action: Using unnatural amino acid mutagenesis, a light-activated zinc-finger nuclease enzyme was engineered through incorporation of a photocaged tyrosine residue at a DNA–protein interface. The caged zinc-finger nuclease was completely inactive until irradiated with UV light, thus enabling photochemical control of sequence specific gene editing in mammalian cells (see picture).

Silicon(II) Compounds

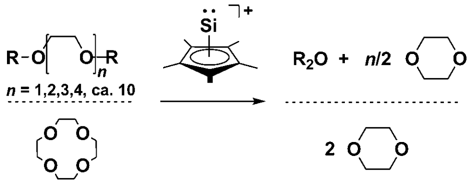

Catalytic open sandwiches: Oligo(ethyleneglycol) diethers $RO(CH_2CH_2O)_nR$ are degraded by the unusual catalyst Cp^*Si^+ (see scheme). The open coordination sphere at silicon allows up to four Si–O contacts; crystal structure data of the reactive compounds $[Cp^*Si(dme)]^+BR_4^-$ and $[Cp^*Si([12]crown\text{-}4)]^+BR_4^-$ ($R = C_6F_5$) show weakly bound ether molecules.

Energy Storage

Impressive energy storage and delivery: A simple, cost-effective, and potentially scalable technique is described for fabricating support- and additive-free NiO/Ni nanocomposite electrodes (see picture) for electrochemical supercapacitors. Maximum performances of energy storage and delivery were simultaneously achieved by developing a slow-charging and fast-discharging procedure.

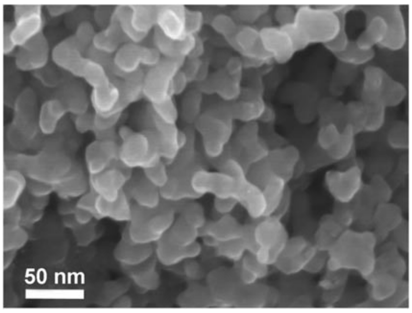

Biosensors

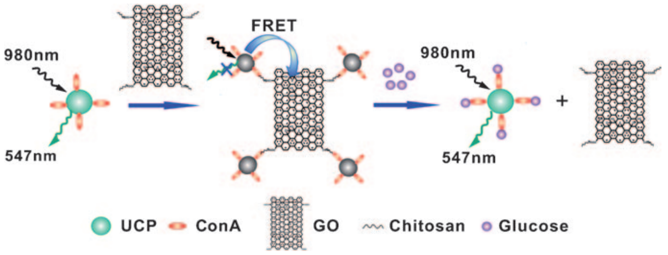

A glucose sensor based on FRET between concanavalin A (ConA)-labeled upconverting phosphor (UCP) nanocrystals and chitosan (CS)-labeled graphene oxide (GO) is presented. Binding of ConA to CS quenches the fluorescence of UCP, which is restored in the presence of glucose, owing to competition between glucose and CS for ConA (see picture).

Porphyrinoids

K. Fujino, Y. Hirata, Y. Kawabe,
T. Morimoto, A. Srinivasan, M. Toganoh,
Y. Miseki, A. Kudo,
H. Furuta* ——— **6855 – 6859**

Confusion and Neo-Confusion: Corrole Isomers with an NNNC Core

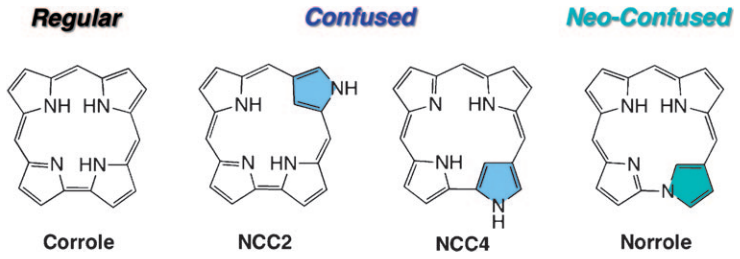

More confused than ever: Three types of N-confused corrole isomers (NCCs) were synthesized, and the structures of these isomers were revealed by single-crystal X-ray crystallography. The position of the confused pyrrole ring in the NCC has a pronounced effect on optical and anion-binding properties.

π-Stacking Interactions

A. S. Jalilov, S. F. Nelsen,* I. A. Guzei,
Q. Wu ——— **6860 – 6863**

Intramolecular π-Stacking Interactions of Bridged Bis-*p*-Phenylenediamine Radical Cations and Diradical Dications: Charge-Transfer versus Spin-Coupling

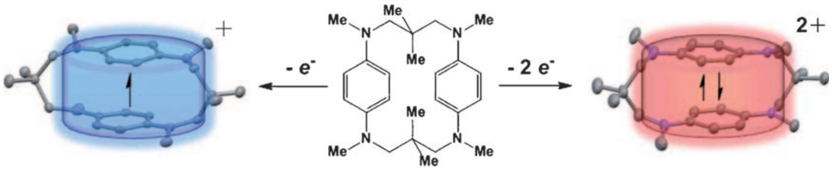

Stacked against the odds: A bridged mixed-valent compound with direct through-space interactions between the charge-bearing units in its singly charged paramagnetic and its doubly charged diamagnetic forms is isolated and characterized by X-ray crystallography and spectroscopy (see scheme). π-Stacking interactions for the singlet diradical dication were more pronounced than for the doublet monocation, despite the Coulomb repulsion effect in the diradical dication.

DNA Photochemistry

Y. Lu, Z. Lan,* W. Thiel* ——— **6864 – 6867**

Hydrogen Bonding Regulates the Monomeric Nonradiative Decay of Adenine in DNA Strands

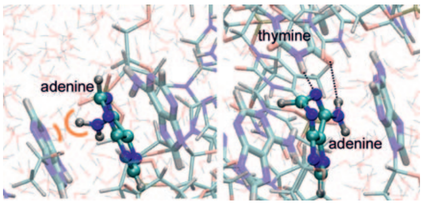

Distinct fates: For adenine in $(dA)_{10}$, the internal conversion to the ground state is dominated by an S_0/S_1 conical intersection with a strong out-of-plane deformation of the amino group (left). In $(dA)_{10}\cdot(dT)_{10}$, this channel is suppressed by adenine–thymine hydrogen bonding (right). The excited-state lifetimes of adenine are computed to be ten times longer in DNA strands than in vacuo or in water.

Contents

Gold Catalysis

D. Lebœuf, A. Simonneau, C. Aubert,
M. Malacria,* V. Gandon,*
L. Fensterbank* ______ **6868 – 6871**

Gold-Catalyzed 1,3-Acyloxy Migration/5-*exo*-dig Cyclization/1,5-Acyl Migration of Diynyl Esters

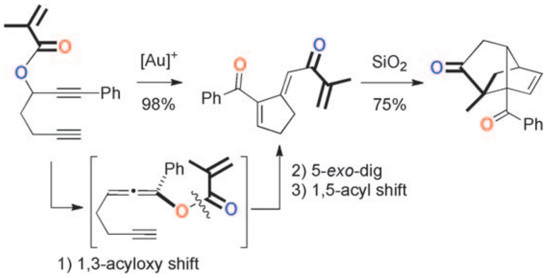

Working three shifts: Polyconjugated δ-diketones are formed stereoselectively in high yields by the gold-catalyzed rearrangement of 1,6-diyn-3-yl esters. This cascade involves a 1,3-sigmatropic acyloxy shift, a 5-*exo*-dig cyclization of the resulting allenyne, and an unprecedented 1,5-sigmatropic shift of an acyl fragment. The usefulness of the products was shown by an efficient acid-catalyzed transformation into a complex polycyclic framework.

Bio-Electrochemistry

M. Hermes, F. Scholz,* C. Härdtner,
R. Walther, L. Schild, C. Wolke,
U. Lendeckel ______ **6872 – 6875**

Electrochemical Signals of Mitochondria: A New Probe of Their Membrane Properties

Current events: Isolated functionally intact mitochondria attach to the hydrophobic surface of a static mercury electrode and disintegrate by forming islands on the surface of the electrode within about 1–2 ms (see picture). The kinetics of this process reveals information on the microfluidity of the mitochondrial membrane.

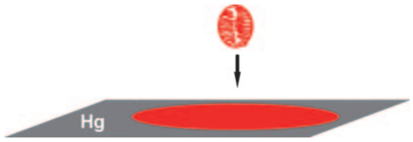

Photoluminescence

J. H. Hao,* Y. Zhang,
X. H. Wei ______ **6876 – 6880**

Electric-Induced Enhancement and Modulation of Upconversion Photoluminescence in Epitaxial $BaTiO_3$:Yb/Er Thin Films

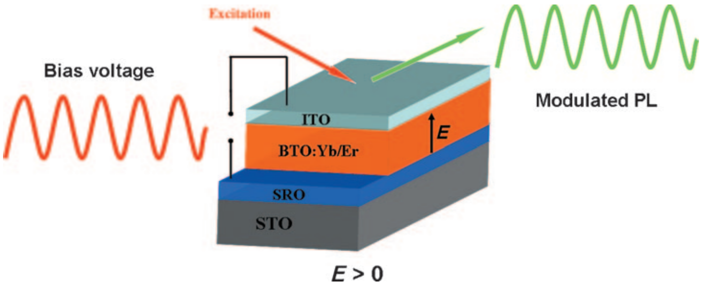

Upconversion control: Applying a relatively low bias voltage to an epitaxial lanthanide-doped $BaTiO_3$ thin film results in a significant enhancement of the upconversion emission. Moreover, the photoluminescence (PL) intensity can be modulated with an ac electric field (see picture). This approach provides a real-time and dynamic way to control photoluminescence.

CO Reduction to Methoxide

A. S. P. Frey, F. G. N. Cloke,* M. P. Coles,
L. Maron, T. Davin ______ **6881 – 6883**

Facile Conversion of CO/H_2 into Methoxide at a Uranium(III) Center

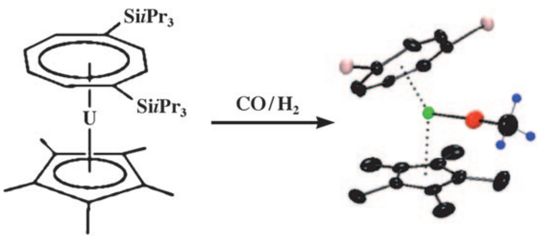

Hydrogenation of CO: The reaction of $[U(\eta\text{-}C_8H_6\{Si\textit{i}Pr_3\text{-}1,4\}_2)(\eta\text{-}Cp^*)]$ in toluene with CO and H_2 at subambient to ambient temperature and pressure affords the methoxide complex $[U(\eta\text{-}C_8H_6\{Si\textit{i}Pr_3\text{-}1,4\}_2)(\eta\text{-}Cp^*)OMe]$.

Conducting Polymers

D. Lepage, C. Michot, G. Liang,
M. Gauthier,
S. B. Schougaard* ———— **6884 – 6887**

A Soft Chemistry Approach to Coating of $LiFePO_4$ with a Conducting Polymer

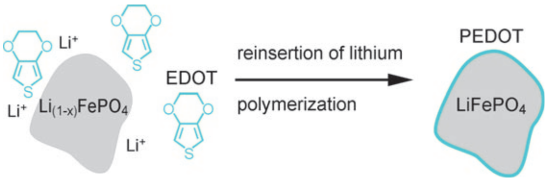

No carbon added: Using the intrinsic oxidative power of $LiFePO_4$/$FePO_4$ combined with the reinsertion of lithium ions, the formation of the conducting polymer poly(3,4-ethylenedioxythiophene) (PEDOT) at the solid surface is demonstrated (see picture). The resulting composites have very promising electrochemical properties in rechargeable lithium batteries; in particular, they allow for the elimination of carbon additives.

C–H Bond Functionalization

K. Gao, N. Yoshikai* ———— **6888 – 6892**

Cobalt–Phenanthroline Catalysts for the *ortho* Alkylation of Aromatic Imines under Mild Reaction Conditions

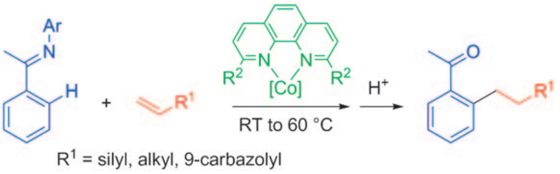

Mild mannered: Cobalt catalysts complexed with phenanthroline-type ligands and activated with Grignard reagents serve as inexpensive and effective catalysts for the *ortho* alkylation of aromatic imines with a variety of olefins (see scheme). The new catalytic systems feature remarkably mild reaction conditions for C–H bond activation and functionalization.

Organocatalysis

M. Moccia, F. Fini, M. Scagnetti,
M. F. A. Adamo* ———— **6893 – 6895**

Catalytic Enantioselective Addition of Sodium Bisulfite to Chalcones

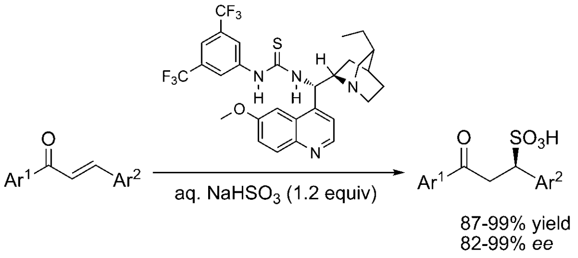

At last! The addition of bisulfite to olefins, discovered over a century ago, remains the most straightforward approach to aliphatic sulfonic acids. A catalytic enantioselective procedure has now been realized that employs a bifunctional aminothiourea catalyst (see picture). Sulfonic acids were obtained from chalcones in high yields and high enantioselectivity and in both configurations.

Palladium Complexes

J. Vicente,* A. Arcas, F. Juliá-Hernández,
D. Bautista ———— **6896 – 6899**

Synthesis of a Palladium(IV) Complex by Oxidative Addition of an Aryl Halide to Palladium(II) and Its Use as Precatalyst in a C–C Coupling Reaction

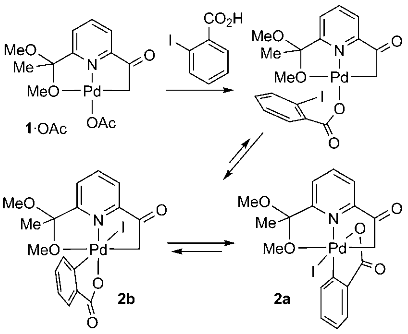

Four’s a charm: Complex **1**·OAc (see scheme) reacts with 2-iodobenzoic acid to afford the stable Pd^{IV} complexes **2a** and **2b**. Complexes **2** are precatalysts for the orthovinylation of 2-iodobenzoic acid with $CH_2{=}CHCO_2Me$ and $AgClO_4$ at room temperature. The reaction is not quenched by excess Hg nor does it afford dibenzyl in the presence of benzyl chloride, suggesting that neither Pd nanoparticles nor a Pd^0 complex are involved.

Contents

Cascade-Reaction Design

W. Liu, V. Khedkar, B. Baskar,
M. Schürmann, K. Kumar* _ **6900 – 6905**

Branching Cascades: A Concise Synthetic Strategy Targeting Diverse and Complex Molecular Frameworks

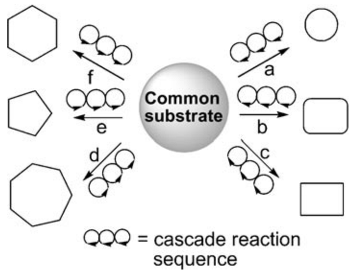

Touch ’n’ transform: A synthetic strategy based on cascade or domino reaction sequences enabled the simultaneous incorporation of skeletal diversity and molecular complexity in focused compound collections. Thus, the treatment of a common multifunctionalized substrate with various cascade-triggering molecules (see picture) generated a wide range of both natural product related and unprecedented molecular frameworks.

Polycyclic Hydrocarbons

A. Shimizu, Y. Tobe* ______ **6906 – 6910**

Indeno[2,1-*a*]fluorene: An Air-Stable *ortho*-Quinodimethane Derivative

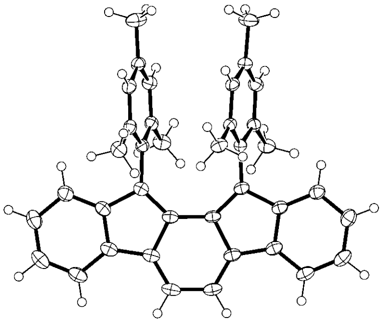

A new isomer: 11,12-Dimesitylindeno[2,1-*a*]fluorene was synthesized and isolated in crystal form. The indenofluorene exhibits significant bond-length alternation in the *o*-quinodimethane structure, limited singlet biradical character, and weakly antiaromatic character. Optical and electrochemical properties suggest that indeno[2,1-*a*]fluorene derivatives may be candidates for optoelectronic materials.

Synthetic Methods

D. Vasu, H.-H. Hung, S. Bhunia,
S. A. Gawade, A. Das,
R.-S. Liu* ______________ **6911 – 6914**

Gold-Catalyzed Oxidative Cyclization of 1,5-Enynes Using External Oxidants

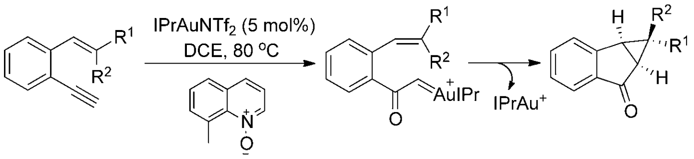

Golden circle: Two gold-catalyzed oxidative cyclizations of 1,5-enynes using 8-methylquinoline *N*-oxide are presented (see example). Experimental results indicate that both reactions proceed through prior oxidation of alkyne to form α-carbonyl intermediates and subsequent intramolecular carbocyclization.

Organocatalysis

B. Maji, M. Breugst,
H. Mayr* ______________ **6915 – 6919**

N-Heterocyclic Carbenes: Organocatalysts with Moderate Nucleophilicity but Extraordinarily High Lewis Basicity

Unique organocatalysts: Arduengo’s carbenes **1** and **2** are 10^3 times more nucleophilic than the Enders carbene **3**, which attacks electrophiles with similar rates as diazabicyclo[5.4.0]undecene (DBU) and 4-(dimethylamino)pyridine (DMAP). The unique organocatalytic activities of **1**–**3** are explained by their extraordinarily high Lewis basicities, which exceed those of PPh_3, DBU, and DMAP by more than 100 kJ mol^{-1}.

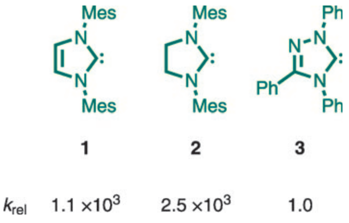

Coexistence of metamagnetism and slow relaxation of magnetization is a very rare phenomenon, which is found in the title compound that is accessible through thermal decomposition reaction of precursors with terminally N-bonded anions and bidentate ligands. The picture shows the relaxation of the magnetism for $H > H_C$.

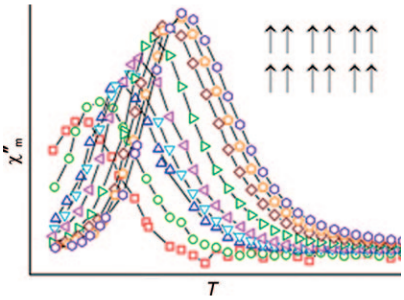

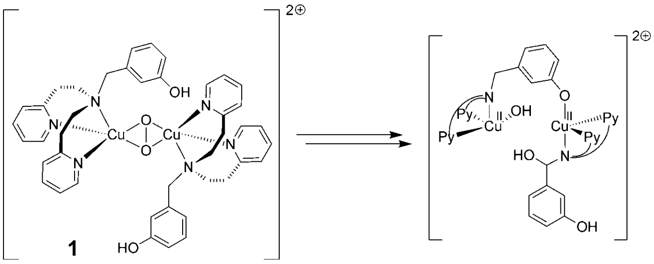

Radicals in directed pathways: The μ-η^2:η^2 peroxo Cu^{II}_2 intermediate **1** shows a much faster benzylic ligand hydroxylation than systems without phenol. This novel reactivity can be further accelerated by addition of external H-atom donors such as TEMPO-H. The results imply initial H-atom transfer leading to the formation of phenoxyl radicals. A highly reactive copper oxyl intermediate is then formed, which inserts oxygen into the benzylic C—H bond.

Supporting information is available on www.angewandte.org (see article for access details).

A video clip is available as Supporting Information on www.angewandte.org (see article for access details).

This article is available online free of charge (Open Access).

Service